Application of Anderson- Schulz- Flory (ASF) Equation in the Product Distribution of Slurry Phase FT Synthesis with Nanosized Iron Catalysts

A. Tavakoli*, M. Sohrabi* and A. Kargari*
*Amirkabir University of Technology, Faculty of Chemical Engineering,
Tehran 15914, Iran, sohrabi@aut.ac.ir

ABSTRACT

Application of ASF equation on the product distribution of FT synthesis using nanosized iron catalysts is studied. The dependencies of product distribution on the reaction temperature and reduction conditions of nanocatalysts are investigated by the growth probability of hydrocarbons (α). The latter has been calculated for three different FT catalysts under various operating conditions and hydrocarbon ranges (n). Since ASF equation may not be suitable for these systems, a new approach has been put forward. According to such an approach the molar product distribution is applied to calculate α values from the slopes of the plots of $\ln(mol\%/n)$ against n. The latter are called the quasi-ASF plots. Quasi-ASF plots follow the same trends as those of ASF but with an improved linearity.

Keywords: Anderson- Schulz- Flory; FT synthesis; nanosized iron catalysts

1 INTRODUCTION

Fischer- Tropsch (FT) synthesis which discovered in 1920s, remains one of the major research topic within alternate fuels R&D due to its applications. FT reaction is the catalytic hydrogenation of carbon monoxide which yields a wide range of alkenes, alkanes, and oxygenated compounds [1-6].

Two classes of reactors are used in the FT process: fixed and fluidized beds. The latter can be subdivided into two-phase (solid and gas) and three- phase (solid, liquid, and gas) or slurry systems. Among these types of reactors, the slurry three- phase catalytic reactor seems to be a better choice due to its advantages [2, 7, 8].

Only the four members of the group VIII, (Fe, Co, Ni, and Ru), have sufficiently high activities for the hydrogenation of carbon monoxide to warrant their use as effective FT catalysts. It is cleared that only cobalt and iron based catalysts may be considered as practical FT catalysts [2]. Iron- based catalyst systems remain the preferred choice in commercial FT synthesis plants [1, 9].

Studies with highly dispersed metals as nanocatalysts are of interest because nanosizing increases surface area that exposes more catalytic sites. In addition, in exothermic reactions such as FT process, nanocatalysts are likely to be more effective and selective or show other interesting properties as the temperature is lowered [3,4, 10].

The molecular mass spread of the FT products can be varied over a wide ranges by changing the operating conditions and/ or the type of catalyst [2,7,11]. The interrelationships between the various FT products are due to the step-wise growth nature of the FT mechanism [2,7]. The details of the FT reaction on a molecular level still remain a controversial matter; nevertheless, in all proposed mechanisms a step-wise growth procedure is assumed [2]. If the hydrocarbon chain is formed step-wise by insertion or addition of C_1 intermediates with constant growth probability (α) then the chain length distribution is given by the ASF distribution [7]. Assuming that α to be independent from hydrocarbon chain length, the derived equation is:

$$\log(W_n / n) = n \log \alpha + const. \qquad (1)$$

where W_n is the mass fraction of the species with carbon number n. From the slope of the plot of $\log(W_n / n)$ against n the value of α is obtained [2]. The majority of the reported ASF plots showed a nearly straight line only in the C_4 - C_{12} region. A number of authors have determined the growth factor from the straight-line portion of the ASF plot. This made the experimental determination of α somewhat arbitrary [12].

However, for most iron, cobalt and ruthenium catalysts marked deviations from this ideal distribution are observed [2,7,12]. In these cases, product distributions can be represented by superposition of two ASF distributions. This bimodal distribution was interpreted by different phenomena [7,12-14]. The product distribution of FT synthesis in bimodal distribution has been characterized by two independent ASF distributions with different chain growth probabilities (α_1, α_2) and the point of intersection of the two ASF distributions. The fraction of methane in total products does not obey the ASF equation due to the several routes of formation. Furthermore ethane can either start or can be incorporated into growing chains. Therefore, the determination of growth probabilities of the bimodal ASF distribution is based on hydrocarbons with carbon numbers greater than two [7].

Calculations have demonstrated that if the range of the assumed values for α is narrow, a single α can adequately describe the molecular weight distribution [12].

The aim of the present study is to investigate the application of ASF equation in the product distribution of FT synthesis with nanosized iron catalysts. Furthermore, the dependencies of product distribution on the reaction

temperature and reduction conditions of nanocatalysts were also investigated. Since there is a few literature studies specifically related to the slurry- phase FT product distribution with nanosized catalysts, the data reported by Mahajan et. al [3,4] have been applied in this study.

Table 1 shows the data summary of FT synthesis runs catalyzed by unsupported nano Fe particles (NANOCAT and BASF) and supported UCI systems [3].

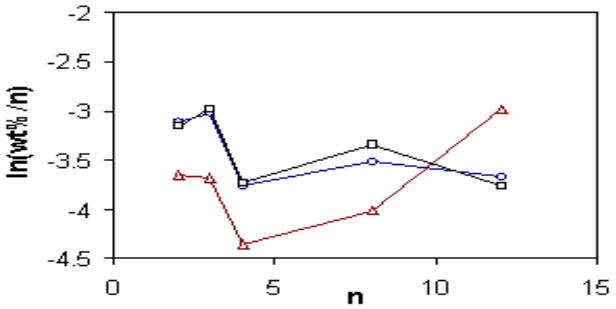

Figure 1: ASF plot of the hydrocarbon distribution obtained during FT synthesis catalyzed by NANOCAT (◇), BASF (□) and UCI (△) catalysts. Reaction conditions are as [4].

To consider the effects of different reduction conditions on product distribution, the ASF plots were drawn for CO and syngas treated NANOCAT catalysts (Fig. 2). Similar to the previous case, C_1 fraction was ignored. The upward shift in the ASF plot of CO treated NANOCAT catalyst, particularly in case of $C_2 - C_8$ range, may demonstrate the higher activity of this catalyst relative to that of syngas treated catalyst. The calculated α and R^2 values in Table 2 showed that the correlation between CO treated NANOCAT catalyst and ASF equation is better than that of syngas treated catalyst and ASF relation. The larger values for α determined in the present study relative to those reported in the literatures [3,4] may be either related to the narrow hydrocarbon range with small n applied in this study, or to the less applicability of ASF equation for these systems.

Another parameter that can affect the product distribution is reaction temperature. ASF plots for NANOCAT catalysts at various reaction temperatures and under different operating conditions were shown in Fig. 3. It is clear from this figure that, with increase in reaction temperature the hydrocarbon products within $C_1 - C_8$ range are also increased. The calculated α and R^2 values with C_1 fraction ignored are shown in Table 2. It is evident that ASF distribution is more accurate within higher reaction temperatures. This may indicate that the step-wise mechanism is predominant at higher reaction temperatures.

In all states mentioned above, it may be observed that ASF plots are not linear, which in turn reflect the dependency of α values on carbon numbers. In order to examine the accuracy of ASF equation for FT product distribution on nanosized iron catalysts, values for α were calculated at different carbon number ranges. To consider

Table 1: Data summary of FT synthesis runs[a] [3]

	NANOCAT			BASF	UCI
T (K)	513	533 [b]	533 [c]	513	513
% conversion					
H_2	34.8	44.7	14.3	41.7	38.7
CO	42.9	52.1	16.2	55.9	65.4
$H_2 + CO$	40.5	46.8	14.9	48.5	47.4
Hydrocarbon product distribution, wt%					
C_1	12.8	16.0	16.4	10.7	7.0
C_2	8.9	11.2	11.4	8.5	5.2
C_3	14.6	15.4	13.8	15.2	0.6
C_4	9.3	11.4	8.8	9.6	5.1
$C_5 - C_{10}$	23.7	30.0	23.0	28.2	14.5
C_{11+}	30.7	16.0	26.6	27.8	60.6
Overall product distribution, wt%					
Hydrocarbon	31.8	32.3	35.9	30.5	28.4
H_2O	36.5	37.2	40.6	30.5	25.0
CO_2	31.7	30.5	23.5	39.0	46.6
STY, kg /(kg-Fe.h)					
$C_1 - C_4$	0.26	0.37	0.09	0.36	0.22
C_{5+}	0.14	0.17	0.04	0.20	0.16

[a] Reaction conditions are as [3]. [b]At P= 2.77 MPa; SV=5.78 $NL/(g-Fe.h)$. [c]Initially reduced with 67% H_2 /33%CO gas mixture. Syngas feed rates during FT synthesis were 6.3 (24 h) and 4.4 (28 h) $NL\ g-Fe^{-1}\ h^{-1}$. Total run time= 52.5 h. Operating P= 2.8 MPa.

Table 2**:** Calculated growth probabilities and R^2 values in different conditions

	wt.%		Mole%	
	α	R^2	α	R^2
T = 513K				
NANOCAT	0.9516	0.3846	0.8060	0.8597
BASF	0.9484	0.4026	0.8033	0.8836
UCI	1.0703	0.3054	0.9065	0.3426
Reduction conditions for NANOCAT				
CO treated	0.8861	0.7545	0.7504	0.9363
Syngas treated	0.9292	0.4937	0.7870	0.8459
Reaction temperatures for NANOCAT				
T=513K	0.9516	0.3846	0.8060	0.8597
T=533K	0.8861	0.7545	0.7504	0.9363

variation of α with the range of hydrocarbon, average values for α ($\overline{\alpha}$), α range width, and standard deviation for different α series in each individual catalyst were calculated and are presented in Table 3. It is evident that α values are widely scattered and R^2 values are so small that the application of ASF equation for FT product distribution have to be approached with cautious.

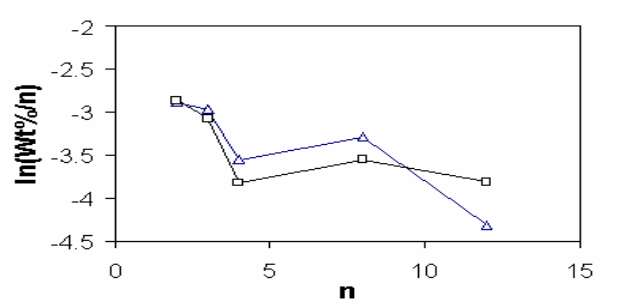

Figure 2: ASF plot obtained during FT synthesis catalyzed by NANOCAT. The initial oxide catalyst precursor was initially reduced with CO (△), and Syngas (□).

To resolve the anomaly, the molar product distribution was considered in the quasi-ASF plots. The latter is in fact a plot of ln(mol%/n) against carbon number. Quasi- ASF plot were drawn for different catalysts (Fig. 4), CO and syngas treated NANOCAT catalysts (Fig. 5), and different reaction temperatures (Fig. 6). The trends of these plots are similar to those of ASF plots, however, with improved linearity. In other words, the quasi-ASF plots can explain the qualitative efficiency of each catalyst similar to ASF, however, the use of molar product distribution in calculation of α may be more accurate (see Table 2). The data in Table 3 show that the deviations of α values from average values determined from quasi-ASF plots are smaller than those calculated using conventional technique. In addition with quasi-ASF approach, the α range width obtained is narrower, the average values for α are closer to those stated in the literature [3,4] and the number of data required is less than those used in ASF calculation.

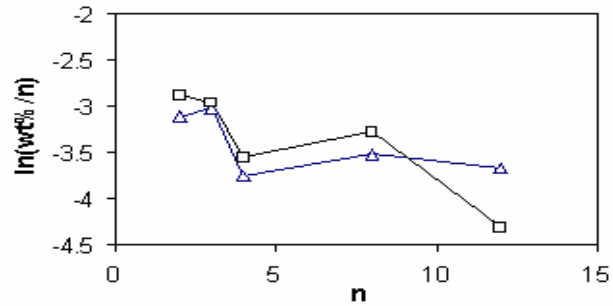

Figure 3: ASF plot obtained during FT synthesis catalyzed by NANOCAT. T=513 K (△), and T=533K (□).

Fig. 7 shows the α value variation as a function of cumulative product distribution on wt.% and mol.% basis. These plots demonstrated that the growth chain probability at certain wt.% and/or mol.% of products is largest for UCI catalyst. This means that the deactivation of UCI catalyst compared to two other catalysts is slower. It is in good agreement with Mahajan et al. data [3,4] for CO and H_2 conversions after 120 h which were 43% and 35% for NANOCAT, 55% and 42% for BASF and, 64% and 37% for UCI, respectively. The faster rate of deactivation of nanocatalysts is understandable due to their larger surface/volume ratios.

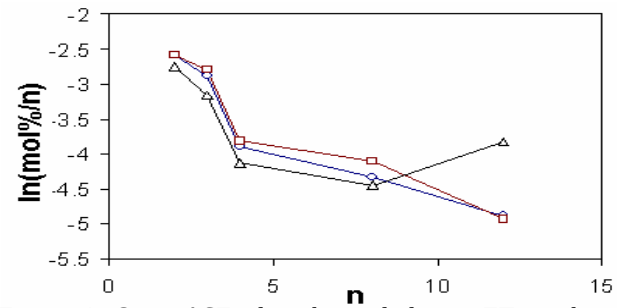

Figure 4: Quasi-ASF plot obtained during FT synthesis catalyzed by NANOCAT (○), BASF (□) and UCI (△) catalysts. Reaction conditions are as [3], T= 513 K.

2 CONCLUSIONS

Since the experimental determination of α is somewhat arbitrary, the calculation of this parameter has been performed at different hydrocarbon numbers as proposed in the literatures. In a particular study the C_1 fraction was considered, while in another case C_2 and C_8 fractions were ignored. In performing the calculations, $C_5 - C_{10}$ and C_{11+} ranges were taken as C_8 and C_{12} hydrocarbons respectively. In all cases considered in the present investigation it was observed that by application of mol per cent instead of weight per cent data, the results obtained were more reasonable, i.e., narrower α range width, meaningful $\overline{\alpha}$, higher regression coefficients, and smaller standard deviation. Furthermore, calculations with nanocatalysts based on mole% led to highly reasonable

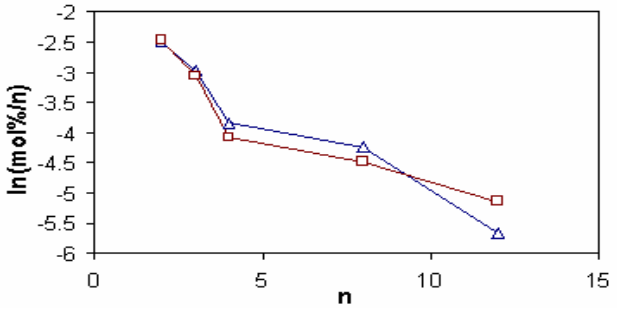

Figure 5: Quasi-ASF plot obtained during FT synthesis catalyzed by NANOCAT. The oxide catalyst precursor was initially reduced with CO (△), and Syngas (□).

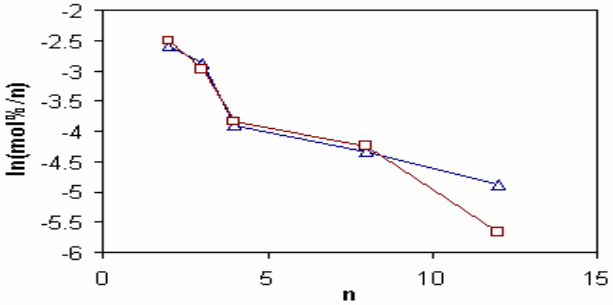

Figure 6: Quasi-ASF plot obtained during FT synthesis catalyzed by NANOCAT. T=513 K (△), and T=533K (□).

Table 3: Calculated growth probabilities and R^2 values in different carbon ranges

	wt.%						Mole%					
	NANOCAT		BASF		UCI		NANOCAT		BASF		UCI	
n	α	R^2	α	R^2	α	R^2	α	R^2	α	R^2	α	R^2
2-3	1.09	1.00	1.19	1.00	0.97	1.00	0.75	1.00	0.81	1.00	0.66	1.00
2-4	0.72	0.65	0.75	0.54	0.70	0.78	0.52	0.91	0.54	0.87	0.50	0.95
2-8	0.93	0.29	1.04	0.09	0.95	0.19	0.75	0.81	0.78	0.76	0.77	0.77
2-12	0.95	0.39	0.95	0.40	1.07	0.31	0.81	0.86	0.80	0.88	0.91	0.34
$d\alpha$ [a]	0.371		0.441		0.370		0.286		0.272		0.403	
$\bar{\alpha}$	0.925		0.983		0.923		0.707		0.734		0.710	
S [b]	0.070		0.102		0.074		0.049		0.051		0.087	

a: α range width = Max α -Min α ; b: $S = \sum_i (\alpha_i - \bar{\alpha})^2$

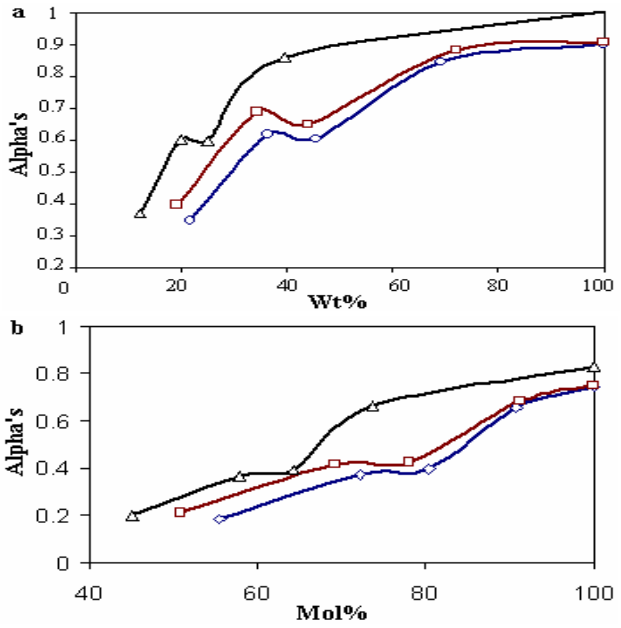

Figure 7: The α values variations as a function of cumulative product distribution, based on wt.% (a) and based on mol.% (b). NANOCAT (○), BASF (□), UCI (△).

results when C_1 fraction was ignored, while in case of weight% data the results were not stable. In other words, in certain cases ,satisfactory results obtained for α , when C_1 fraction was considered such as syngas treated NANOCAT catalyst, while in some other circumstances reasonable results were found by ignoring C_2 and C_8 fractions, such as CO treated NANOCAT catalyst. Dependency of α values on hydrocarbon numbers is noteworthy and shows that ASF equation may be not suitable for nanoparticle catalyst systems and may indicate that different growth mechanisms may be dominant during hydrocarbon synthesis with nanocatalysts. Another advantage of molar calculation is the need for less hydrocarbon ranges data while the results of such calculations are close to α values based on mass per cent calculations [3,4] by taking into account some larger ranges of hydrocarbons data.

Referring to figures 1 and 7 and Table 3, it may be observed that the BASF catalyst for FT process seems to be more active in comparison with that of UCI. In addition, the BASF catalyst's stability is higher than that of NANOCAT catalyst.

REFRENCES

[1] H. Schulz, Appli. Catal. A 186, 3, (1999).

[2] Istvan T. Horvath, Encyclopedia of Catalysis, John Wiley & Sons, Fischer- Tropsch Synthesis-Industrial, Vol 3, 347-403, (2003).

[3] D. Mahajan, P. Gutlich, J. Ensling, K. Pandya, U. Stumm, and P. Vijayaraghavan, Energy and Fuels 17, 1210, (2003).

[4] D. Mahajan, P. Gutlich, and U. Stumm, Catal. Commun. , 4, 101, (2003).

[5] M. Ahmadi M., M. Sohrabi, S. Zarrinpashne, and G. Baghmisheh, Chem. Eng. Technol., 28, 78, (2005).

[6] B. C. Dunn, D. J. Covington, P. Cole, R. J. Pugmire, H. L. C. Meuzelaar, R. D. Ernst, E. C. Heider, and E. M. Eyring; Energy and Fuels, 18, 1519, (2004).

[7] J. Patzlaff, Y. Liu, C. Graffmann, J. Gaube., Appli. Catal. A, 186, 109, (1999).

[8] V. R. Ahon, E. F. Costa Jr., J. E. P. Monteagudo, C. E. Fontes, E. C. Biscaia Jr., P. L. C. Lage, Chem. Eng. Sci., 60, 677, (2005).

[9] R. L. Espinoza, A. P. Steynberg, B. Jager, A. C. Vosloo, Appli. Catal. A, 186, 13, (1999).

[10] C. Burda, X. Chen, R. Narayanan, and M. A. El-Sayed, Chem. Rev., 105, 1025, (2005).

[11] W. D. Deckwer, R. Kokuun, E. Sanders, and S. Ledakowicz, Ind. Eng. Chem. Process Des. Dev., 25, 643, (1986).

[12] I. Puskas, and R. S. Hurlbut, Catal. Today, 84, 99, (2003).

[13] J. Patzlaff, Y. Liu, C. Graffmann, J. Gaube, Catal. Today, 71, 381, (2002).

[14] X. Zhan, B. H. Davis, Appli. Catal. A, 236, 149, (2002).